

## Article

# Development and Application of a Nano-Gas Sensor for Monitoring and Preservation of Ancient Books in the Library

Jia Wang <sup>1,\*</sup>, Qingyu Wang <sup>2</sup>, Susu He <sup>2</sup>, Zhiyin Chen <sup>2</sup>, Wentong Qiu <sup>2</sup> and Yunjiang Yu <sup>2</sup><sup>1</sup> Library, Lingnan Normal University, Zhanjiang 524048, China<sup>2</sup> Key Laboratory of Advanced Coating and Surface Engineering, Lingnan Normal University, Zhanjiang 524048, China; qingyuwang@163.com (Q.W.); hesusudemao@163.com (S.H.); chizhiyin2023@163.com (Z.C.); q13560545805@163.com (W.Q.); sidui@lingnan.edu.cn (Y.Y.)

\* Correspondence: wangjia@lingnan.edu.cn

**Abstract:** Monitoring the gas composition in library environments is crucial for the preservation of ancient books. In this study, TiO<sub>2</sub> NTs/CNTs composites were synthesized via a hydrothermal method and utilized as nano-gas sensors for NO<sub>2</sub> detection. The surface morphology and element composition of the samples were characterized using scanning electron microscopy (SEM) and energy dispersive spectroscopy (EDS). Additionally, the gas sensitivity of the prepared TiO<sub>2</sub> nanocomposites was evaluated at different temperatures, both with and without ultraviolet light irradiation. The results demonstrate that the synthesized TiO<sub>2</sub> NTs/CNTs samples exhibit a large specific surface area due to their titanium dioxide nanotubes (TiO<sub>2</sub> NTs) and carbon nanotubes (CNTs) composition. Moreover, these samples display excellent gas sensitivity under ultraviolet light irradiation at temperatures of 120 °C. Compared to uncomposited and non-ultraviolet light irradiated samples, the sensor response rate is significantly improved, enabling effective monitoring of NO<sub>2</sub> gas in library environments conducive to preserving ancient books. Overall, our findings highlight that the developed TiO<sub>2</sub> NTs/CNTs nano gas sensor holds great potential for monitoring and safeguarding ancient books.

**Keywords:** TiO<sub>2</sub> nanotubes; hydrothermal method; book protection; gas-sensitive sensor



**Citation:** Wang, J.; Wang, Q.; He, S.; Chen, Z.; Qiu, W.; Yu, Y. Development and Application of a Nano-Gas Sensor for Monitoring and Preservation of Ancient Books in the Library. *Coatings* **2024**, *14*, 553. <https://doi.org/10.3390/coatings14050553>

Academic Editor: Octavian Buiu

Received: 21 March 2024

Revised: 20 April 2024

Accepted: 23 April 2024

Published: 30 April 2024



**Copyright:** © 2024 by the authors. Licensee MDPI, Basel, Switzerland. This article is an open access article distributed under the terms and conditions of the Creative Commons Attribution (CC BY) license (<https://creativecommons.org/licenses/by/4.0/>).

## 1. Introduction

As a crucial component of cultural heritage, ancient books and literature embody the legacy and evolution of exceptional traditional culture. To ensure their continuous preservation, significant time and effort must be invested [1]. Comprehensive protection of ancient bookstores necessitates monitoring internal corrosive and oxidizing gases. NO<sub>2</sub> dissolves in water to form nitric acid, which not only exhibits acidity but also strong oxidation potential. Acidic conditions can degrade paper cellulose, leading to book acidification, while the potent oxidizing properties of NO<sub>2</sub> can cause oxidative decomposition of paper cellulose [2]. Detection methods for these gases encompass selected ion flow tube mass spectrometry, gas chromatography–mass spectrometry, proton transfer reaction mass spectrometry, and gas sensor detection technology [3,4]. Among these, gas sensor detection technology is gaining popularity due to its affordability and ease of use [5]. Therefore, developing rapid and accurate NO<sub>2</sub> gas sensors with low cost, low power consumption, and excellent sensitivity is critical for gas-monitoring equipment in ancient bookstores.

The types of gas sensors primarily include electrochemical, contact combustion, light reaction, and metal-oxide semiconductor (MOS) gas sensors. Among these, MOS gas sensors have garnered significant attention due to their advantageous features such as portability, high sensitivity, good stability, and low preparation cost [6]. MOS sensors have been used to detect toxic and harmful gases in libraries, but the problems of low sensitivity and high operating temperature have not been completely solved. TiO<sub>2</sub> exhibits ultra-high chemical stability, non-toxicity, and excellent thermal stability at elevated temperatures. It finds extensive application in the field of gas-sensitive sensor research; however, TiO<sub>2</sub>

suffers from a wide band gap (3.2 eV) and low efficiency when utilizing natural light [7]. Carbon nanotubes (CNTs) possess remarkable chemical stability, mechanical durability, exceptional electrical properties, and an extremely high specific surface area. Moreover, the electrical characteristics of CNTs are easily influenced by favorable changes in surface adsorption [8], while their gas sensitivity can be enhanced under ultraviolet light irradiation [9]. Consequently, employing CNTs as sensing materials in gas sensors can yield heightened sensitivity towards electrons or gases with strong electron-withdrawing properties (e.g.,  $\text{NH}_3$  gas and  $\text{NO}_2$  gas) even at room temperature. Zhao et al. synthesized  $\text{In}_2\text{O}_3$  nanowires through solvothermal method, which showed a high response value of 54.6 to 1 ppm  $\text{NO}_2$  at 150 °C [10]. Liu et al. utilized the atomic layer deposition to prepare sensor fabricated on nanotubes, which exhibited good response and acceptable response time of 65 s to 0.5 ppm  $\text{NO}_2$  under UV illumination [11]. However, the above reported methods for nanostructured materials have weaknesses of intricate manipulation, the usage of UV illumination and noble metals also increases in sensor costs [12]. Hence, It is necessary to invent the  $\text{NO}_2$  sensor that can quickly and sensitively detect the trace amount of  $\text{NO}_2$  in the air at low operating temperature.

In this manuscript, we employed a low-cost hydrothermal method and non-metallic doping technique to synthesize composite products of  $\text{TiO}_2$  nanotubes/C nanotubes ( $\text{TiO}_2$  NTs/CNTs). The gas sensing properties of the composite products were systematically investigated under different temperatures and ultraviolet light irradiation. By incorporating heterostructures and employing photoactivation techniques, significant improvements in the gas sensing performance are achieved [13,14]. Moreover, we developed a gas sensor based on multidimensional nanostructures to improve its sensitivity and lower the detection temperature for  $\text{NO}_2$  gas, thereby effectively reducing the risk of damage to ancient books stored in libraries.

## 2. Materials and Methods

### 2.1. Preparation of $\text{TiO}_2$ NTs and $\text{TiO}_2$ NTs/CNTs

To start, 2 g  $\text{TiO}_2$  nanoparticles and 80 mL 10 M NaOH solution were added to the beaker, and they were transferred to the reaction kettle for hydrothermal reaction at 130 °C for 24 h with ultrasonic stirring for 30 min each. The solution was washed to neutral and the precipitation was taken out and stirred in 5% HCl solution for 1 h. The white precipitation was washed to neutral, dried at 70 °C for several hours, and calcined at different temperatures to obtain  $\text{TiO}_2$  NTs. The CNTs were ultrasonically dissolved in an alcohol solution and magnetically stirred for 30 min to form a uniform CNT solution (0.1 mg/mL).  $\text{TiO}_2$  nanoparticles, HCl solution, CNTs, sodium hydroxide (NaOH), and absolute ethanol ( $\text{CH}_3\text{CH}_2\text{OH}$ ) were purchased from Sinopharm Chemical Reagent Co., Ltd. (Shanghai, China) without further purification.

Deionized water was added to the beaker, followed by the addition of titanium dioxide, carbon nanotubes, and sodium hydroxide in sequence. To achieve homogeneity, the solution was stirred using a magnetic stirrer for 30 min. Subsequently, ultrasonic treatment was conducted on the solution for 30 min to obtain a mixed solution which was then transferred into a 100 mL liner and placed inside a reaction kettle. The reaction kettle was positioned in a drying oven set at 150 °C for hydrothermal reaction. After 24 h, the reaction concluded and the bottom layer of the liner was extracted as the first composite product [15]. Subsequently, it was soaked in 30 mL of dilute hydrochloric acid with pH adjusted to 1 for another 24 h. Further centrifugal cleaning ensured neutralization before drying and grinding were carried out. The ground powder underwent calcination in a muffle furnace set at 400 °C for two hours, resulting in obtaining a  $\text{TiO}_2$  NTs/CNTs composite product. The final product contained about 3% carbon nanotubes, and experimental tests have shown that it exhibits excellent gas sensing properties.

## 2.2. Characterization of TiO<sub>2</sub> NTs/CNTs

The morphology of the sample was observed and analyzed using scanning electron microscopy (SEM/EDS, SU3800, Hitachi-Hightech, Tokyo, Japan). X-ray diffraction (XRD, RINT2000) was employed to analyze the phase of TiO<sub>2</sub> NTs/CNTs. In XRD measurements, a Ni-filtered Cu source with a wavelength of 1.54 nm (K $\alpha$ ) was used to generate X-rays and the measurements were taken between 10° and 90° with a step size of 0.01°.

## 2.3. Fabrication of Gas Monitoring Sensors

The gas-sensing device was custom-built based on the description provided in a previous publication [14]. Firstly, grind the sample and set it aside. Next, place the fork finger electrode into the sample bottle and extract 10 g of the ground sample. Add anhydrous ethanol to the sample bottle and subject it to ultrasonic treatment for 10 min, resulting in a suspension of the sample in anhydrous ethanol. Subsequently, heat the sample in a water bath to evenly precipitate it onto the fork finger electrode. The resistance of the sample is measured using a multi-function electricity meter, with only components exhibiting resistance at M $\Omega$  level considered as gas-sensitive components. We employed a self-built gas-sensitive test bench consisting of an air-expelling system, an air-filling system, a test chamber, tungsten steel needles, a heating table, gas-sensitive components, a resistance tester, and a computer (Figure 1). To initiate testing procedures, insert the fork finger electrode into the vacuum chamber while crossing pairs of tungsten steel needles.

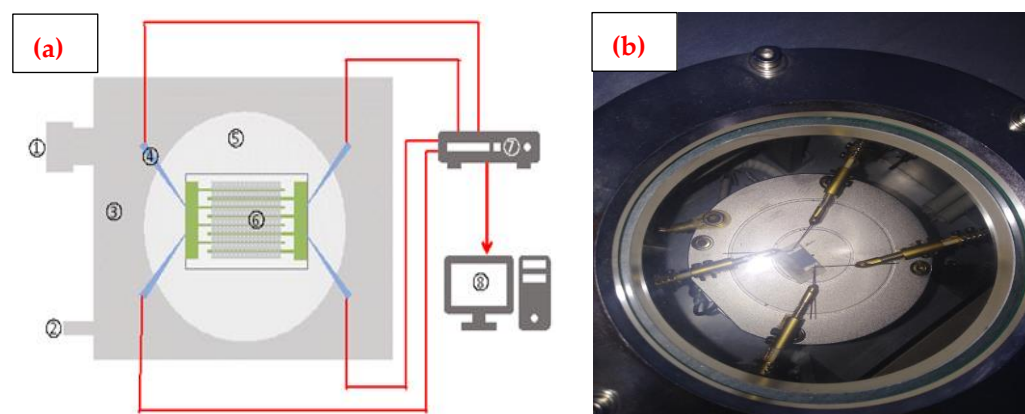


**Figure 1.** (a) Schematic diagram of vacuum gas sensitivity test system: exhausting system; ① Vacuum pumping system; ② aeration system; ③ test chamber; ④ tungsten steel needle; ⑤ heating platform; ⑥ gas sensitive element; ⑦ resistance tester; ⑧ computer. (b) The picture of the manufactured sensor based on TiO<sub>2</sub> NTs/CNTs.

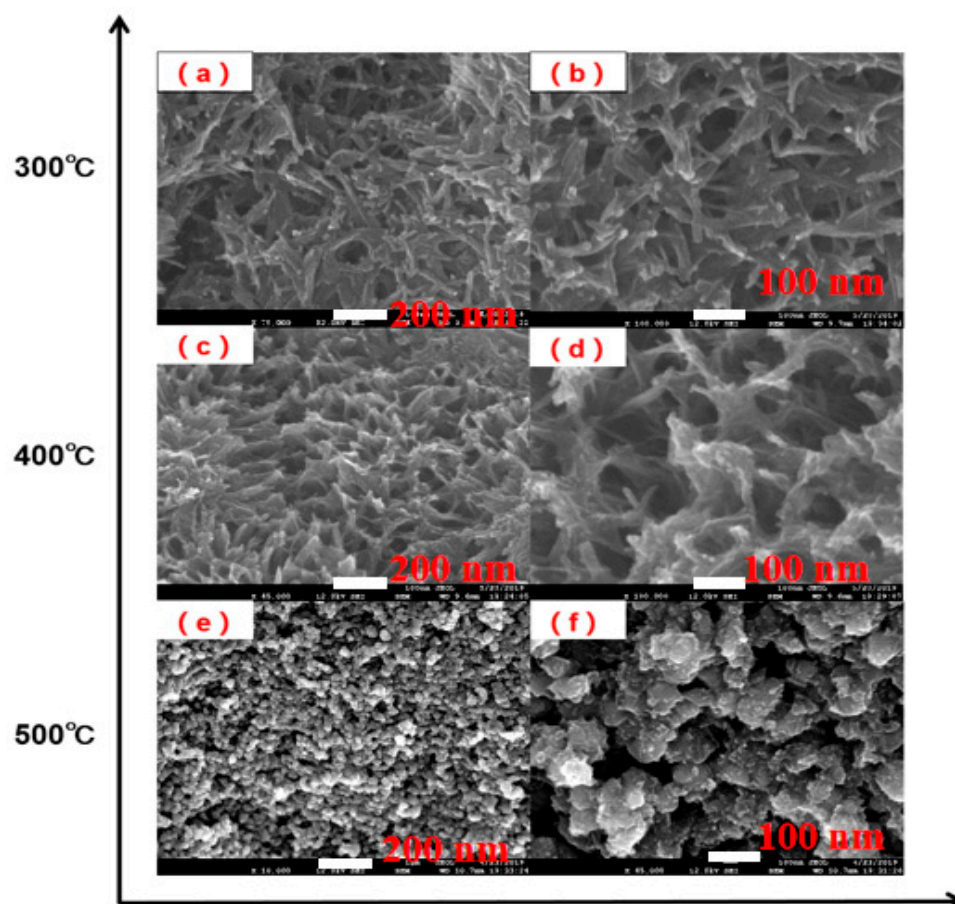
The central gas-sensitive element is irradiated with UV light (365 nm), and a temperature controller controls the experimental environment. The test gas from the gas source is controlled for flow rate and total input using a D07–19BM mass flow controller (sevenstar, Beijing, China) and a D08–8CM flow meter (sevenstar, Beijing, China). The change in the resistance value is received and transmitted using the Keithley Model 2450 digital source meter (Tektronix Inc., Beaverton, OR, USA) by the vacuum four-probe resistance testing system. After the set parameters reach a stable value, the gas-sensitive material is tested for gas sensing. The resistance change curve is obtained by detecting the resistance value before and after introducing the gas. The measurement was conducted at room temperature ( $T = 25.0 \pm 0.5$  °C) and dry air (relative humidity (RH) =  $15.5 \pm 1.7\%$ ) during the test.

## 3. Results and Discussion

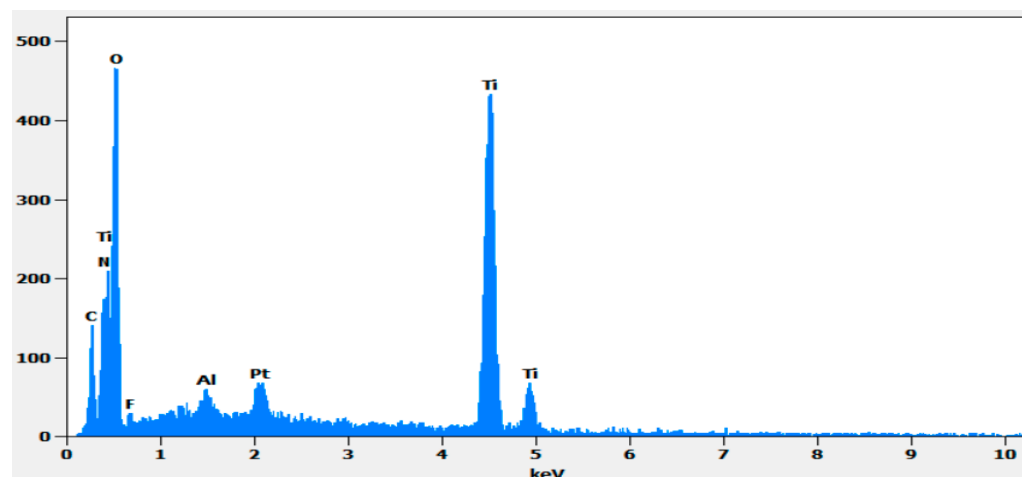
### 3.1. Morphology and Phase Analysis of TiO<sub>2</sub> NTs/CNTs

Figure 2 illustrates the surface morphology of the sample at different calcination temperatures. As depicted, at a calcination temperature of 300 °C, the TiO<sub>2</sub> NTs/CNTs

product exhibits a disordered tubular structure with some unformed accumulations still present. At a calcination temperature of 400 °C, compared to the product calcined at 300 °C, a significant number of intertwined TiO<sub>2</sub> NTs and CNTs are observed in the product, forming numerous pore structures that result in a larger specific surface area for TiO<sub>2</sub> NT/CNTs. However, when the temperature reaches 500 °C, the nanotube morphology of TiO<sub>2</sub> NTs/CNTs completely disappears and the sample transforms into nanoparticles with a diameter above 30 nm. As can be seen from EDS images shown in Figure 3, the weight ratio of carbon nanotubes to TiO<sub>2</sub> was found to be 3%.



**Figure 2.** SEM images of TiO<sub>2</sub> NTs/CNTs with different calcination temperatures: (a,b) 300 °C; (c,d) 400 °C; (e,f) 500 °C.



**Figure 3.** EDS images for TiO<sub>2</sub> NTs/CNTs with calcination temperatures of 300 °C.

As depicted in Figure 4, TiO<sub>2</sub> NTs exhibit a prominent diffraction peak at  $2\theta = 27.45^\circ$  [16], corresponding to the crystal structure of TiO<sub>2</sub> (110). Notably, as illustrated in the figure, an increase in calcination temperature leads to a progressively sharper characteristic diffraction peak for anatase, indicating enhanced crystallization with elevated calcination temperatures. Simultaneously, it can be observed from the figure that when calcination temperature is below 500 °C, hydrothermally treated TiO<sub>2</sub> NTs lack the rutile diffraction peak. This suggests that rutile-phase formation does not occur in TiO<sub>2</sub> NTs under calcination temperatures below 500 °C and implies complete destruction of the rutile–anatase (P90) structure of raw material by strong alkali solution. Energy spectrum analysis of the composite product comprising TiO<sub>2</sub> NTs/CNTs reveals presence of titanium (Ti), carbon (C), and oxygen (O), confirming stoichiometric proportionality within the composite product. In Figure 4b, all diffraction peaks are consistent with the peak positions of TiO<sub>2</sub> nanotubes. The sharpness of the diffraction peaks indicates that the crystallinity of TiO<sub>2</sub> remains high in the presence of carbon nanotubes. However, no distinct characteristic peaks of carbon nanotubes are observed in the figure, indicating that in cases where the content is only 3% and 5%, the disorderly accumulation of carbon nanotubes causes significant damage, resulting in relatively small or even absent diffraction peaks.

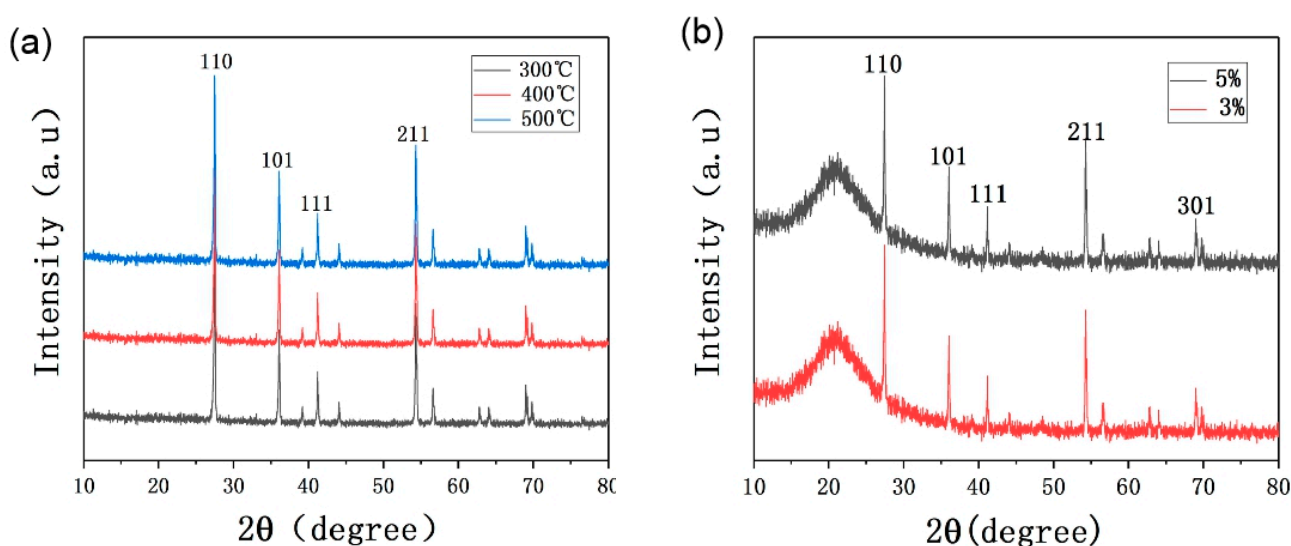


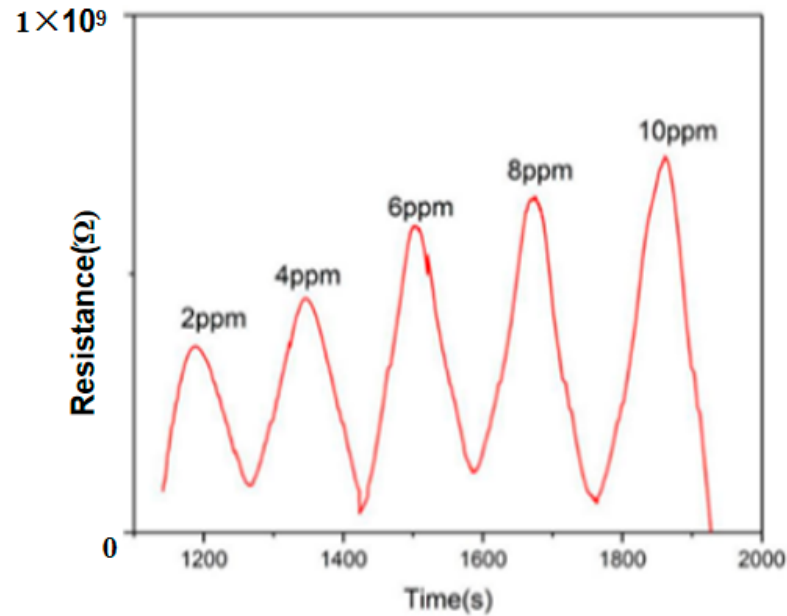
**Figure 4.** XRD patterns of TiO<sub>2</sub> NTs with different calcination temperatures (a) and TiO<sub>2</sub> NTs/CNTs with CNTs contents of 3% and 5% (b).

### 3.2. Gas-Sensitive Properties of TiO<sub>2</sub> NTs/CNTs

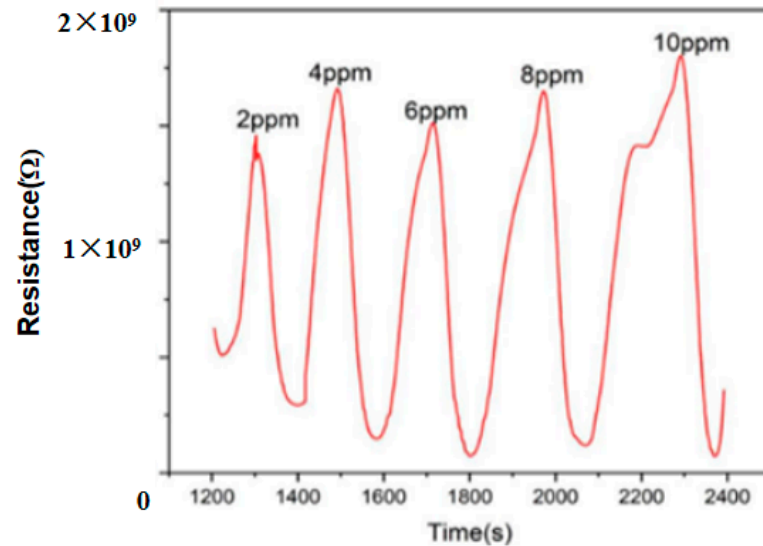
The gas-sensing response of the devices to oxidizing gases can be defined as  $S = R_g/R_a$ , where  $R_g$  and  $R_a$  represent the resistance of the gas sensor in the detected gas and air, respectively. The response time and recovery time were defined by the time for the gas sensor to achieve 90% of the total response change with the exposure and evacuation of the detected gases, respectively. The response recovery curves of TiO<sub>2</sub> material with NO<sub>2</sub> gas concentrations of 2, 4, 6, 8, and 10 ppm are presented in Figure 5. The resistance of the material shows minimal change after exposure to NO<sub>2</sub> gas. The sensor exhibits a gas-sensing response of approximately 1. At 10 ppm, the sensor demonstrates maximum gas-sensing response with a response time of 91 s and a recovery time of 84 s. This study selected this as the research basis to test whether the response time and recovery time of TiO<sub>2</sub> NTs/CNTs nanocomposites to NO<sub>2</sub> gas at different temperatures were improved, and whether the gas-sensitive response of the sensor was improved.

The response recovery curves of the TiO<sub>2</sub> NTs/CNTs nanocomposites following exposure to 2, 4, 6, 8, and 10 ppm NO<sub>2</sub> gas at 120 °C exhibited an enhanced gas-sensing response compared to Figure 5. As shown in Figure 6, the nanocomposites displayed the best response to 8 ppm NO<sub>2</sub> gas with a gas-sensing response of 2.28, a response time of 97 s,

and a recovery time of 225 s. In comparison to pure  $\text{TiO}_2$  materials without nanocomposites products, both the response time and recovery time are prolonged by about 6 s and 171 s, respectively, compared to Figure 5. However, the gas-sensing response of the sensor is increased by 1.3 times.

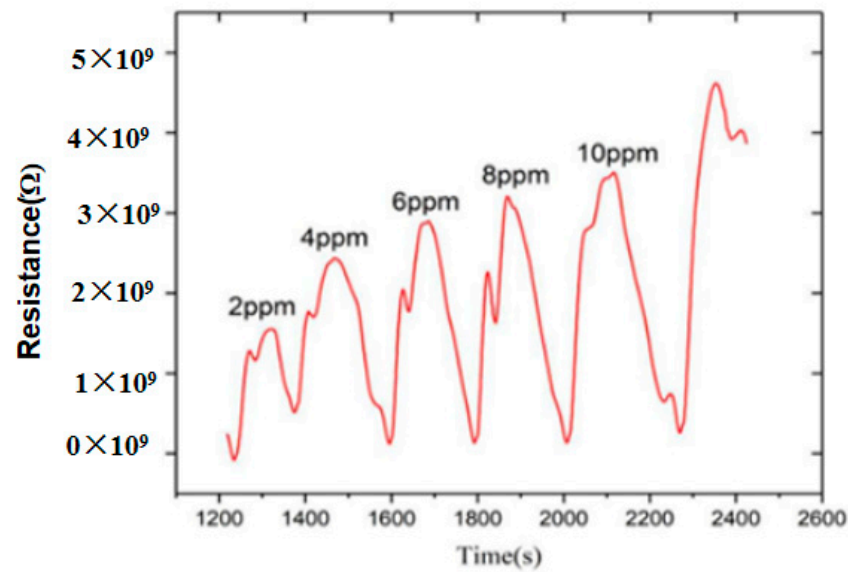


**Figure 5.** The response–recovery curves of  $\text{TiO}_2$  at temperatures of  $120\text{ }^\circ\text{C}$  subsequent to the introduction of  $\text{NO}_2$  gases at concentrations of 2, 4, 6, 8, and 10 ppm.



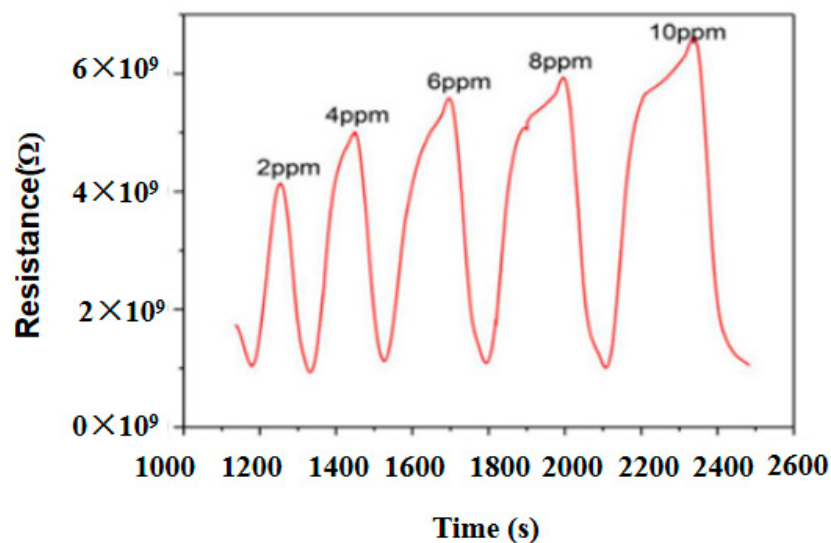
**Figure 6.** Response recovery curves of  $\text{TiO}_2$  NTs/CNTs nanocomposites at  $120\text{ }^\circ\text{C}$  and with concentrations of 2, 4, 6, 8, and 10 ppm.

Figure 7 shows the gas response recovery curve of  $\text{TiO}_2$  NTs/CNTs in response to  $\text{NO}_2$  with concentrations of 2, 4, 6, 8, and 10 ppm at  $200\text{ }^\circ\text{C}$ . With the increase in  $\text{NO}_2$  gas concentrations, the gas-sensing response of the sensor reaches the maximum value of 12 at 10 ppm, and the response time is 163 s. The response time is extended by 66 s and the recovery time is 107 s compared with that at  $120\text{ }^\circ\text{C}$ , and the recovery time is reduced by 85 s. Compared with pure  $\text{TiO}_2$  materials, although the response time and recovery time are slightly longer, the gas-sensing response of the sensor is greatly improved.



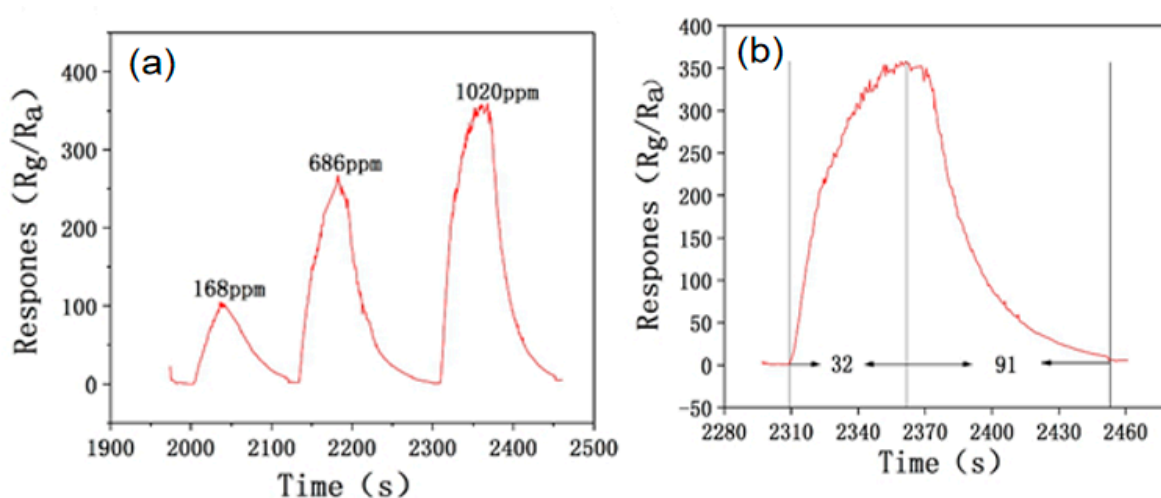
**Figure 7.** The recovery curve of TiO<sub>2</sub> NTs/CNTs in response to successive introduction of NO<sub>2</sub> with different concentrations at a temperature of 200 °C.

Figure 8 shows the response recovery curve of TiO<sub>2</sub> NTs/CNTs materials at 120 °C with NO<sub>2</sub> gas concentrations of 2, 4, 6, 8, and 10 ppm under ultraviolet irradiation. As can be seen from the figure, the gas-sensing response of the sensor increases with the increase in NO<sub>2</sub> gas concentrations, and reaches the maximum value when the gas concentration is 10 ppm ( $S = R_a/R_g = 6.57$ ). The response time of the sensor is 234 s, and the recovery time is 133 s. Compared with sensors without UV irradiation at 120 °C, the gas-sensing performance is significantly improved, and the gas-sensing response is increased by about six times, although the response time and recovery time are prolonged. Compared with sensors without ultraviolet irradiation at 200 °C, the gas-sensing response decreased, and the response time and recovery time were relatively long. The response time and recovery time were extended by 71 s and 26 s compared with 200 °C without ultraviolet irradiation, which failed to achieve good gas-sensitive performance under low temperature and ultraviolet irradiation at the same time. This shows that at the same temperature, the gas sensitive performance of the sensor can be improved under ultraviolet irradiation, but the response recovery time cannot be shortened by ultraviolet irradiation [17].



**Figure 8.** The response recovery curve of TiO<sub>2</sub> NTs/CNTs under ultraviolet light irradiation at 120 °C after introduction of NO<sub>2</sub> ranging from 2 to 10 ppm.

The continuous transient response recovery of the TiO<sub>2</sub> NTs array to NO<sub>2</sub> at different temperatures is shown in Figure 9. The test demonstrates that the TiO<sub>2</sub> NTs array exhibits excellent selectivity for NO<sub>2</sub> at a temperature of 320 °C [18]. As depicted in Figure 9a, when the temperature is set at 320 °C and the concentration of NO<sub>2</sub> increases from 168 to 1020 ppm, the response value of the TiO<sub>2</sub> NTs array to NO<sub>2</sub> rises from 100 to 400. Upon removal of the NO<sub>2</sub>, the resistance of the TiO<sub>2</sub> NTs array increases and returns to its original state. This not only suggests that higher concentrations enhance sensitivity for detecting NO<sub>2</sub> gas but also highlights good reversibility exhibited by TiO<sub>2</sub> NTs. Even after multiple repeated operations, the response value can still return to its initial level. As illustrated in Figure 9b, when exposed to a concentration of 1020 ppm of NO<sub>2</sub>, it takes approximately 32 s for TiO<sub>2</sub> NTs to respond, indicating a favorable response value towards NO<sub>2</sub> gas at both a temperature of 320 °C and this particular concentration level. However, it requires around 90 s for complete recovery due to a strong linear correlation between the resistance of the nanocomposites and NO<sub>2</sub> gas concentration during this process [19].



**Figure 9.** (a) Transient response recovery of TiO<sub>2</sub> NTs/CNTs to 168, 686, and 1020 ppm NO<sub>2</sub> gas at 320 °C; (b) transient response of TiO<sub>2</sub> NTs array to 1020 ppm NO<sub>2</sub> gas at 320 °C.

As shown in Figure 10, the curve showed a relatively stable trend during a long-term stability measurement of 30 days toward 8 ppm NO<sub>2</sub> gas. Moreover, after 30 consecutive tests, no apparent decrease trend in response was observed for detecting 8 ppm NO<sub>2</sub>. These results demonstrate that the TiO<sub>2</sub> NTs/CNTs-based sensor possesses good repeatability and long-term stability. In addition, the effects of environmental factors such as humidity, temperature fluctuations, and light exposure on the sensors are currently in the process for optimizing experimental parameters. The properties of TiO<sub>2</sub> NTs/CNTs heterojunction nanostructure are potentially superior to their individual component because of greater active sites for adsorption of the target gas, which means a higher response.

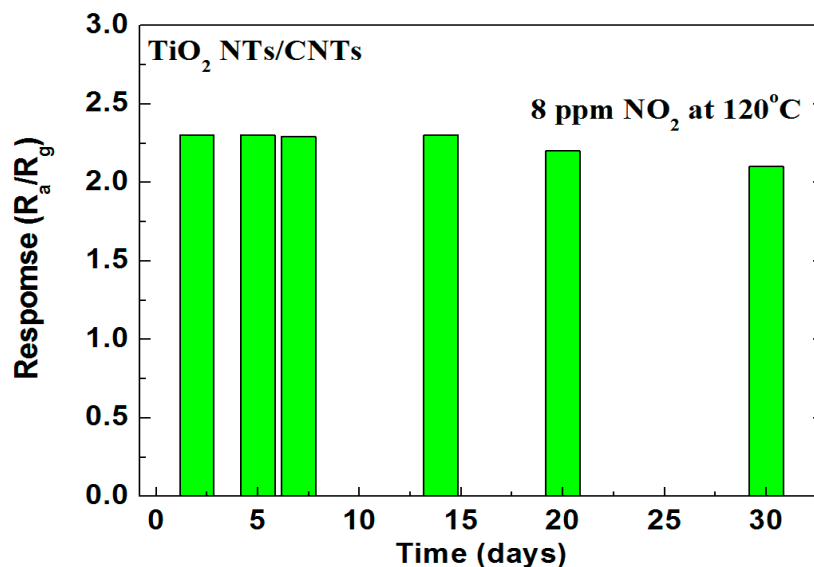


Figure 10. Stability test during a long-term of 30 days toward 8 ppm NO<sub>2</sub> gas.

#### 4. Gas-Sensitive Reaction Mechanism

The gas monitoring can be explained by the combination of the adsorption–desorption model [20] and the energy band theory [21]. Firstly, TiO<sub>2</sub> NTs array acts as an N-type semiconductor. In this study, a non-metallic material P-type semiconductor material CNT is selected for doping on the basis of a TiO<sub>2</sub> NTs array. After doping, a heterojunction PN junction is formed at the interface of these two materials [21]. Moreover, electrons are carriers in N-type semiconductors and participate in conduction while holes are carriers in P-type semiconductors and also participate in conduction. As electrons move from an N-type semiconductor TiO<sub>2</sub> NTs to P-type semiconductor CNTs, TiO<sub>2</sub> NTs become positively charged whereas holes move from P-type semiconductor CNTs to N-type semiconductor TiO<sub>2</sub> NTs resulting in negative charge accumulation on CNTs. Consequently, an electric field is established at the heterojunction which increases the Schottky barrier leading to the excellent gas-sensitive performance of the TiO<sub>2</sub> NTs/CNT composite [22]. Owing to the relative position of the CNT and TiO<sub>2</sub> CB edge [19], the electrons injected into the oxide can be shuttled into the graphitic network, as proposed for photo-injected carriers in TiO<sub>2</sub>/CNTs catalysts [23]. Such a process finally brings about a reduction in the h<sup>+</sup> concentration in the CNTs, thus causing the electrical resistance of the nanocomposite to increase [24]. Upon contact with oxidizing gases (such as NO<sub>2</sub>), strong electron absorption occurs on the surface of CNTs causing tilting effect towards oxidizing gases. On a macroscopic scale, this results in a charge transfer between gas molecules and CNT surfaces, increasing hole carrier concentration and conductivity while losing electrons, thus enhancing sensitivity of CNT towards oxidizing gases [25].

#### 5. Conclusions

In this study, TiO<sub>2</sub> NTs/CNTs composites were synthesized via a hydrothermal method and utilized as nano gas sensors for NO<sub>2</sub> detection. A heterojunction junction is formed at the interface of hydrothermal synthesis of TiO<sub>2</sub> NTs and CNT nanocomposites, which increases the Schottky barrier leading to an excellent gas-sensitive performance. This improves the power and sensitivity of the sensor. Increasing calcination temperature enhances the crystal structure of TiO<sub>2</sub> NTs, resulting in increased sensitivity towards NO<sub>2</sub> gas detection with higher concentrations. At 200 °C, the sensor exhibits a 12-fold increase in power compared to 120 °C. Furthermore, under UV irradiation conditions, significant improvements are observed in the material's gas-sensing performance compared to non-irradiated conditions at similar temperatures. However, increasing temperature and adding UV irradiation prolong both response and recovery times relative to initial values for this

gas-sensitive sensor. This study has the potential to decrease production expenses and this sensor can be potentially applied for rapidly and precisely detecting NO<sub>2</sub> in air quality monitoring. Future work will focus on optimizing test parameters for real-time monitoring of ancient book environments to enable timely and efficient protective measures.

**Author Contributions:** Formal analysis, J.W.; Investigation, J.W., Q.W., S.H., Z.C., W.Q. and Y.Y.; Writing—original draft, J.W. All authors have read and agreed to the published version of the manuscript.

**Funding:** This research was funded by Science and Technology Project of Zhanjiang (2022B01044, 2022A0100) and Special Fund for Science and Technology Innovation Strategy in Guangdong Province (pdih2022b0319).

**Institutional Review Board Statement:** Not applicable.

**Informed Consent Statement:** Not applicable.

**Data Availability Statement:** Data are contained within the article.

**Conflicts of Interest:** The authors declare no conflict of interest.

## References

1. Shen, H. Research on the Protection Measures of Ancient Books in University Libraries in the New Era. *J. Northwest Adult Educ. Coll.* **2022**, *1*, 99.
2. Lu, A. Harmful gases in the air to books and their relationship with the humidity of the library. *Nandu Xuetao* **1997**, *2*, 96–97.
3. Borowik, P.; Adamowicz, L.; Tarakowski, R.; Siwek, K.; Grzywacz, T. Odor detection using an E-nose with a reduced sensor array. *Sensors* **2020**, *20*, 3542. [[CrossRef](#)] [[PubMed](#)]
4. Tomic, M.; Setka, M.; Vojkuvka, L.; Vallejos, S. VOCs sensing by metal oxides, conductive polymers, and carbon-based materials. *Nanomaterials* **2021**, *11*, 552. [[CrossRef](#)]
5. Mu, S.; Shen, W.; Lv, D.; Song, W.; Tan, R. Inkjet-printed MOS-based MEMS sensor array combined with one-dimensional convolutional neural network algorithm for identifying indoor harmful gases. *Sens. Actuators A Phys.* **2024**, *369*, 11520. [[CrossRef](#)]
6. Shi, X.; He, Y.; Gong, T.; Xie, Y.; Chen, J.; Yang, X. Preparation of three-dimensional ZnO nanoflowers and their gas sensing performance to indoor polluted gases. *Sens. Microsyst.* **2022**, *41*, 10–13.
7. Xie, L. *Study on Metal-Modified Nano TiO<sub>2</sub> and Its Gas Sensing Performance*; Nanjing University of Aeronautics and Astronautics: Nanjing, China, 2021.
8. Xu, J.; Chen, Y.; Li, Y.; Shen, J. Application of one-dimensional nanomaterials in gas sensors. *Sens. Technol.* **2005**, *1*, 4–6.
9. Chen, G.; Paronyan, T.M.; Pigos, E.M.; Harutyunyan, A.R. Enhanced gas sensing in pristine carbon nanotubes under continuous ultraviolet light illumination. *Sci. Rep.* **2012**, *2*, 343. [[CrossRef](#)] [[PubMed](#)]
10. Zhao, S.; Shen, Y.; Zhou, P.; Hao, F.; Xu, X.; Gao, S.; Wei, D.; Ao, Y.; Shen, Y. Enhanced NO<sub>2</sub> sensing performance of ZnO nanowires functionalized with ultra-fine In<sub>2</sub>O<sub>3</sub> nanoparticles. *Sens. Actuators B Chem.* **2020**, *308*, 127729. [[CrossRef](#)]
11. Liu, Y.; Zhang, J.; Li, G.; Liu, J.; Liang, Q.; Wang, H.; Zhu, Y.; Gao, J.; Lu, H. In<sub>2</sub>O<sub>3</sub>-ZnO nanotubes for the sensitive and selective detection of ppb-level NO<sub>2</sub> under UV irradiation at room temperature. *Sens. Actuators B Chem.* **2022**, *355*, 131322. [[CrossRef](#)]
12. Dang, T.; Nguyen, T.T.O.; Truong, T.H.; Le, A.T.; Nguyen, T.D. Facile synthesis of different ZnO nanostructures for detecting sub-ppm NO<sub>2</sub> gas. *Mater. Today Commun.* **2020**, *22*, 100826. [[CrossRef](#)]
13. Liang, Y.; Wang, H.; Sanchez Casalongue, H.; Chen, Z.; Dai, H. TiO<sub>2</sub> nanocrystals grown on graphene as advanced photocatalytic hybrid materials. *Nano Res.* **2010**, *3*, 701–705. [[CrossRef](#)]
14. Li, M.; Zou, C.; Liang, F.; Hou, E.; Lin, J. Preparation and gas-sensing performance under photoactivation of TiO<sub>2</sub> nanotubes/carbon nanotubes/ZnS quantum dots gas-sensitive materials. *Mater. Today Commun.* **2023**, *36*, 106487. [[CrossRef](#)]
15. Guo, R.-B. *Preparation of g-C<sub>3</sub>N<sub>4</sub> Composite Nanomaterials and Their Photocatalytic Performance*; Nanchang Hangkong University: Nanchang, China, 2018.
16. Huang, D.-G.; Mo, Z.-H.; Quan, S.-Q.; Yang, T.-Z.; Liu, Z.-B.; Liu, M. Preparation and photocatalytic reduction performance of graphene/nano-TiO<sub>2</sub> composites. *Acta Mater. Compos. Sin.* **2016**, *33*, 155–162.
17. Giampiccolo, A.; Tobaldi, M.D.; Leonardi, G.S.; Murdoch, B.J.; Seabra, M.P.; Ansell, M.P.; Ansell, M.P.; Neri, G.; Ball, R.J. Sol gel graphene/TiO<sub>2</sub> nanoparticles for the photocatalytic-assisted sensing and abatement of NO<sub>2</sub>. *Appl. Catal. B Environ.* **2019**, *243*, 183–194. [[CrossRef](#)]
18. Tong, X. *Preparation and Gas Sensing Performance of TiO<sub>2</sub> Nanotube Array Membranes for the Main Components of Papermaking Pollution Gases*; South China University of Technology: Guangzhou, China, 2017.
19. Li, J.; Lu, Y.; Ye, Q.; Cinke, M.; Han, J.; Meyyappan, M. Carbon Nanotube Sensors for Gas and Organic Vapor Detection. *Nano Lett.* **2023**, *3*, 929–933. [[CrossRef](#)]
20. Chang, J.; Jiang, D.-G.; Zhan, Z.L.; Song, W.H. Overview of semiconductor metal oxide gas sensing materials. *Sens. World* **2003**, *9*, 14–18.

21. Tian, K. *Construction of Metal Oxide Semiconductor Heterojunction and Its Gas Sensing and Photoelectrochemical Performance and Mechanism*; Beijing University of Chemical Technology: Beijing, China, 2023.
22. Santangelo, S.; Faggio, G.; Messina, G.; Fazio, E.; Neri, F.; Neri, G. On the hydrogen sensing mechanism of Pt/TiO<sub>2</sub>/CNTs based devices. *Sens. Actuators B* **2013**, *178*, 473–484. [[CrossRef](#)]
23. Xu, Y.J.; Zhuang, Y.; Fu, X. New insight for enhanced photocatalytic activity of TiO<sub>2</sub> by doping carbon nanotubes: A case study on degradation of benzene and methyl orange. *J. Phys. Chem. C* **2010**, *114*, 2669–2676. [[CrossRef](#)]
24. De Luca, L.; Donato, A.; Santangelo, S.; Faggio, G.; Messina, G.; Donato, N.; Neri, G. Hydrogen sensing characteristics of Pt/TiO<sub>2</sub>/MWCNTs composites. *Int. J. Hydrogen Energy* **2012**, *37*, 842–851. [[CrossRef](#)]
25. Lee, J.H.; Kim, J.Y.; Nam, M.S.; Mirzaei, A.; Kim, H.W.; Kim, S.S. Synergistic effect between UV light and PANI/Co<sub>3</sub>O<sub>4</sub> content on TiO<sub>2</sub> composite nanoparticles for room-temperature acetone sensing. *Sens. Actuators B Chem.* **2023**, *375*, 132868–132879. [[CrossRef](#)]

**Disclaimer/Publisher’s Note:** The statements, opinions and data contained in all publications are solely those of the individual author(s) and contributor(s) and not of MDPI and/or the editor(s). MDPI and/or the editor(s) disclaim responsibility for any injury to people or property resulting from any ideas, methods, instructions or products referred to in the content.